JMEPEG (2012) 21:927–935
DOI: 10.1007/s11665-011-9984-2

1059-9495/$19.00

Optimizing Friction Stir Welding via Statistical Design of Tool Geometry and Process Parameters

C. Blignault, D.G. Hattingh, and M.N. James

(Submitted February 22, 2010; in revised form May 12, 2011)

This article considers optimization procedures for friction stir welding (FSW) in 5083-H321 aluminum alloy, via control of weld process parameters and tool design modifications. It demonstrates the potential utility of the "force footprint" (FF) diagram in providing a real-time graphical user interface (GUI) for process optimization of FSW. Multiple force, torque, and temperature responses were recorded during FS welding using 24 different tool pin geometries, and these data were statistically analyzed to determine the relative influence of a number of combinations of important process and tool geometry parameters on tensile strength. Desirability profile charts are presented, which show the influence of seven key combinations of weld process variables on tensile strength. The model developed in this study allows the weld tensile strength to be predicted for other combinations of tool geometry and process parameters to fall within an average error of 13%. General guidelines for tool profile selection and the likelihood of influencing weld tensile strength are also provided.

Keywords destructive testing, quality control testing, welding

1. Introduction

Previous investigations have shown that the measurement of tool forces, temperature and torque during friction stir welding (FSW) is a valuable aid in better understanding and characterization of process dynamics (Ref 1-7). Such measurements facilitate optimized process control and efficient tool design, in turn leading to more efficient and faster welding which is characterized by reduced tool forces, torque and temperature and high mechanical property values.

Once process data can be monitored and recorded reliably, it is possible to use statistical techniques to explore tool and joint optimization. The use of process forces as a statistical process control tool during FSW has also been previously highlighted by Arbegast (Ref 4). The present authors developed a rotating transducer that measures lateral forces during welding and that is attached directly to the spindle of a milling machine that has been converted to a FSW platform. The system records real-time measurements of process variables close to the tool and its main components are a sensing element, tool holder, telemetry system and data-logger as illustrated in Fig. 1. The design, development and calibration procedure of the system has previously been reported in the literature (Ref 1, 5, 7). The system allows real-time assessment of the influences of modifications to tool geometry and to changes in process parameters such as tool feed and speed, either continuously or at various points along the weld seam. Such information could greatly reduce the current high level of empiricism involved in choosing FSW parameters.

Welding forces on the tool can be presented in the form of a lobed polar plot as a function of tool angle during rotation, whose area is related to energy input during welding. Figure 2 shows a typical polar plot of the bending force on the tool acting opposite to the direction of travel of the tool. This force is measured during each rotation of the tool, referenced to a particular position (in the present case the 270º position as shown in Fig. 2). It provides a 2D representation of the maximum and minimum bending force vectors experienced by the tool during each revolution. A similar polar plot can be obtained for the transverse bending force and hence a resultant force plot can also be produced. This "force footprint" (FF) has been proposed (Ref 5, 6) to present a graphical indication of aspects of the macroscopic plastic flow processes of entrainment, mixing and forging during tool rotation. It is believed that these effects are manifested in the area of the plots, and the magnitude and angular rotation of the lobe apogees. The FF

Abbreviations	
FF	force footprint
FS	friction stir
FSW	friction stir welding
GRM	general regression model
GUI	graphical user interface
NRF	National Research Foundation
RSM	response surface model
UTS	ultimate tensile strength
NMMU	Nelson Mandela Metropolitan University

C. Blignault—Deceased.

C. Blignault, D.G. Hattingh, and **M.N. James**, Faculty of Engineering, the Built Environment & Information Technology, Nelson Mandela Metropolitan University, Port Elizabeth 6001, South Africa; and **M.N. James**, School of Marine Science & Engineering, University of Plymouth, Drake Circus, Plymouth, Devon PL4 8AA, UK. Contact e-mails: Danie.hattingh@nmmu.ac.za and mjames@plymouth.ac.uk.

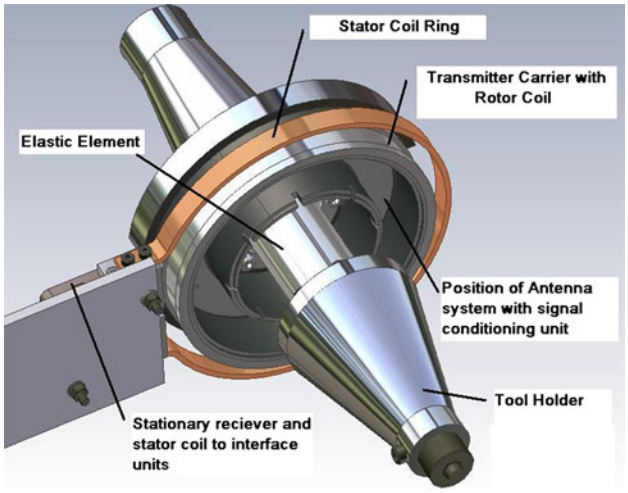

Fig. 1 The monitoring system illustrating the basic telemetry components, tool holder and transducer configuration

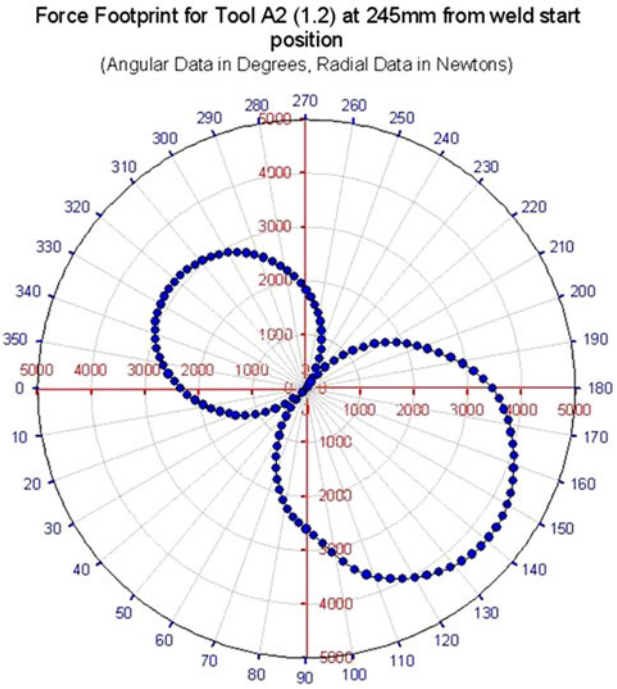

Fig. 2 The profile of a typical force-footprint, which is a polar plot of the maximum and minimum bending force in the welding direction experienced by the tool, as a function of tool rotation angle relative to a fixed position (270°)

hence has the potential to be used in a graphical user interface (GUI) as a simple indicator of "optimum" process conditions for a particular alloy, yet virtually no published study has covered this ability of this concept to predict weld strength as a function of tool geometry and process parameters.

The study reported in this article is novel in that it has demonstrated the potential for a priori prediction of the effectiveness of various changes in tool geometry in achieving desirable mechanical properties in FS welds. It has utilized the measured weld parameters (downwards *z*-force, temperature and torque), in combination with information on the FF lobe apogee (maximum and minimum bending force and lobe rotation/angle)

Table 1 Process input conditions used for all FS welds

Plunge spindle speed	600 rpm
Weld length	340 mm
Plunge feed rate	10 mm/min
Plunge depth (from center of pin)	0.1 mm
Dwell time	8 s
Feed rate	150 mm/min
Weld spindle speed	500 rpm
Tool tilt angle	2.5°
Plate thickness	6 mm
Parent material	5083-H321
Pin length	5.7 mm
The same conical shoulder design was used for all tools	

to establish the viability of using the FF as a GUI for process optimization. The study was performed on a comprehensive matrix of 24 different tool geometries, and data for the six independent process parameters was recorded during welding. A standard statistical analysis using the response surface model (RSM) was then performed to predict weld tensile strength.

2. Experimental Design

The responses of six independent process (or explanatory) variables were measured and used as predictors (regressor variables) in the development of an empirical model to predict weld ultimate tensile strength (UTS) in 6 mm 5083-H321 aluminum alloy. The chosen regressor variables were downwards *z*-force (kN), tool torque (Nm), tool pin temperature (°C), maximum and minimum values of bending force (N-indicated by the terms Max and Min later in the article) experienced by the tool during a revolution, and angular shift of the apogee point of the FF (°) during welding. These variables were measured whilst making two replicate 340 mm long welds for each of the 24 tool geometries. Replicate welds were intended to provide an indication of weld-to-weld error and 4 tensile test specimens were machined from each weld. Table 1 gives the fixed tool geometry and process conditions used for all the FS welds. The tool design matrix is given in Table 2 while Fig. 3 shows the layout of the mechanical property test specimens in relation to a weld run.

3. Prediction Model for Tensile Strength

The innovative aspect of this study is the use of the FF and the force values induced during welding to predict the influence of geometric tool parameters. This is the first necessary step in developing a real-time GUI that would depict optimized welding conditions for a given alloy. Assessment of the viability of this approach requires a statistical analysis of the experimental data. This has been done using standard techniques, whose use in this research is clearly outlined below. In the research use of statistical techniques it is important for other workers to be able to assess the validity of the techniques used, as well as the reported outcomes and hence the technique used in this study is described in some detail.

The prediction of weld tensile strength has been approached through a RSM. This is a general regression model (GRM) technique which explores the relationships between several

Table 2 Changes in tool parameter geometry in each of the six tool series tested

Tool matrix				Geometric parameter (equal % change from 1 → 4)
D1	D2	D3	D4	Depth of flute increased in 1 mm steps. Cutter and pin diameter = 10 mm; offset between cutter and pin center lines changed from 6.5 to 3.5 mm. 25 threads/in. anticlockwise
F1	F2	F3	F4	Flute scallop angle, relative to center-line of pin, increased in 10° steps. Cutter diameter 6 mm, pin diameter 10 mm; scallop angle increased from 10° to 40°. 25 threads/in. anticlockwise
T1	T2	T3	T4	Tool taper angle increased by decreasing tip diameter in 1 mm steps from 8 to 5 mm. Pin diameter 10 mm. 25 threads/in. anticlockwise
A1	A2	A3	A4	Number of flutes increased from 1 to 4; constant pin diameter of 10 mm, cutter diameter of 5 mm and flute depth of 2 mm. 25 threads/in. anticlockwise
P1	P2	P3	P4	Pin diameter decreased in 2 mm steps from 12 to 6 mm. 25 threads/in. anticlockwise
H1	H2	H3	H4	Number of threads/in. increased in steps of 4 tpi, from 16 threads/in. to 28 threads/in.

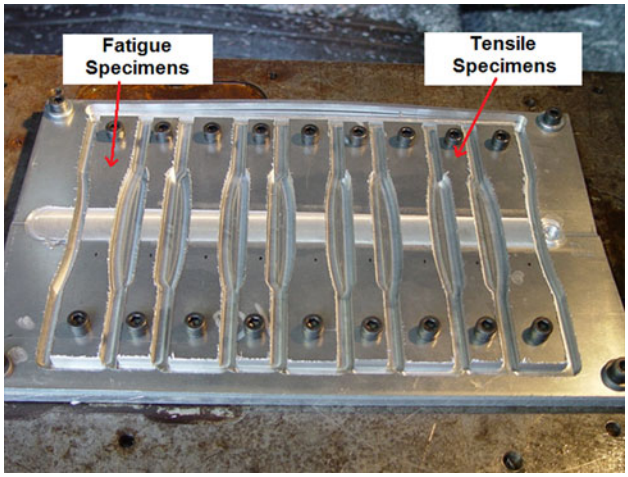

Fig. 3 Layout of tensile and fatigue specimens relative to the FS welds

independent or "explanatory" variables and one or more dependent or response variables. The main idea of RSM is to use a sequence of designed experiments to obtain an optimal response and it is known to be effective in developing, improving and optimizing processes by means of experimental data (Ref 8).

A quadratic response surface regression was used which allows modeling of the two-way interaction effects of the predictor variables. The general form of second-order regression equation for a quadratic response surface regression model, which gives a value for the response variable Y for a continuous or categorical predictor $\boldsymbol{x}$, is given by (Ref 8):

$$Y = b_1 f_1(x) + \cdots + b_p f_p(x) + \varepsilon \quad \text{(Eq 1)}$$

The response is modeled as a linear combination of (not necessarily linear) functions of the predictor, plus a random error ε. The expressions $f_j(x)$ ($j = 1, \ldots, p$) are the *terms* of the model. The β_j ($j = 1, \ldots, p$) are the *coefficients*. Errors ε are assumed to be uncorrelated and distributed with mean value of zero and constant (but unknown) variance.

Input data for this equation was acquired from the 96 "training" samples (4 tensile specimens for each of 24 tool geometries). The response data were evaluated using the Statistica 6 software package by means of the backward removal technique which filters out insignificant variables and less important two-way interactions. The analysis of the model provided a value for multiple $R = 0.904855$, multiple $R^2 = 0.818762$ and adjusted $R^2 = 0.792559$. R is a linear correlation coefficient that indicates the strength of the relationship between the response and explanatory variables and R^2 measures the percent of variation in the response variable that can be accounted for through the explanatory variables. Thus an adjusted R^2-value of 0.79 indicates that the prediction model can predict the response variable (tensile strength) with an accuracy of almost 80% and the relatively small variation between R^2 and adjusted R^2 indicates that only statistical significant variables are contributing in the model.

In a regression analysis each explanatory variable leads to an estimated coefficient representing its importance, an error on the estimate, and a t-value which is the ratio of the estimate divided by the standard error. In Statistica, the Pareto chart function (Fig. 4) provides a useful visual summary of these effects and highlights the most important among a set of influential factors via a histogram showing the relative importance of the factors coupled with a plot showing the cumulative percentage total of the influence of the factors. The chart in Fig. 4 shows the absolute values of the most statistically significant effects or relationships that influence the prediction of the output response (UTS), and are ranked in decreasing order of influence.

In statistical analyses, the p-value represents a decreasing index of the reliability of a result. The higher the p-value, the less likely it is that the observed relationship between explanatory and response variables is a reliable indicator of the relationship between the variables across the whole population. Specifically, the p-value represents the probability of error in accepting the observed result as valid, or representative of the total population. Hence a p-value of 0.05 indicates that there is a 5% probability that the relationship observed between the variables is a result of chance. The dashed vertical line in Fig. 4 represents a 5% level of statistical significance (p-value = 0.05). Those factors whose effects have a higher significance than this value (lower p-value) are therefore primarily responsible for changes in the response variable (UTS) with a 95% $(1 - p)$ confidence level. The analysis identified that 13 factors (or interactions) were statistically significant out of the possible 27. These combinations are listed below in decreasing order of statistical significance but all are still within the 95% confidence interval.

1. Max * Angle—(Maximum bending force multiplied by lobe rotation angle)
2. z-Force * Angle—(Downward z-force multiplied by the lobe rotation angle)

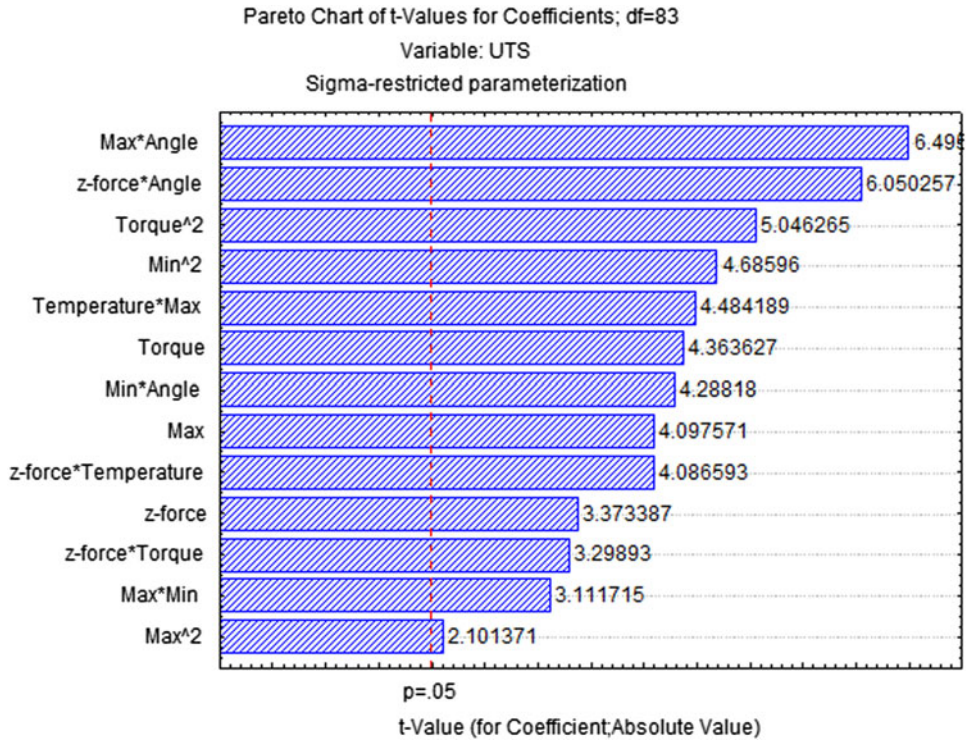

Fig. 4 Pareto chart/histogram of *t*-values for the backward removal method in the GRM

3. Torque^2—(Tool torque squared)
4. Min^2—(Minimum bending force squared)
5. Temperature * Max—(Tool pin temperature multiplied by the maximum bending force)
6. Torque—(Tool torque)
7. Min * Angle—(Minimum bending force multiplied by the lobe rotation angle)
8. Max—(Maximum bending force)
9. *z*-force * Temperature—(Downward *z*-force multiplied by the tool pin temperature)
10. *z*-force—(Downward *z*-force)
11. *z*-force * Torque—(Downward *z*-force multiplied by the tool torque)
12. Max * Min—(Maximum bending force multiplied by the minimum bending force)
13. Max^2—(Maximum bending force squared)

Examination of the histogram given in Fig. 4 indicates that the strongest influences in the model are the maximum bending force on the tool and the angle at which this occurs during a revolution of the tool. These parameters are clearly related to aspects of the plastic entrainment and flow round the tool during welding. Both these parameters and their variation are readily depicted using the FF diagram and thus it could indeed provide a useful GUI in choosing process input parameters (tool rotational speed and feed rate) suitable for making high performance welds. High performance in FS welds relies on optimizing the plastic deformation processes that govern mechanical properties and performance.

These 13 parametric relationships were then incorporated into a model to predict weld UTS. Despite the length of the predictive equation, high performance computers make real-time prediction of weld quality relatively straightforward, provided that the values of the explanatory variables can be accurately measured. The final quadratic RSM for the prediction of weld UTS is given in Eq 2.

$$\begin{aligned}\text{UTS (MPa)} &= 169.129255(Z_f) + 17.2220574(T) - 0.29258887T^2 \\ &\quad - 0.47428050(B_{max}) - 0.31632 \times 10^{-4}(B_{max})^2 \\ &\quad - 0.78022 \times 10^{-4}(B_{min})^2 + 1.20288857(Z_f)(T) \\ &\quad - 0.43520643(Z_f)(t) + 0.001119846(t)(B_{max}) \\ &\quad - 0.87330 \times 10^{-4}(B_{max})(B_{min}) + 0.767810425(Z_f)(\Theta) \\ &\quad - 0.00651537(B_{max})(\Theta) - 0.00462030(B_{min})(\Theta)\end{aligned} \quad \text{(Eq 2)}$$

In Eq 2, Z_f is the downwards *z*-force in kN, t is temperature in °C, T is torque in Nm, B_{max} is the maximum bending force in N, B_{min} is the minimum value of bending force in N, and Θ is lobe rotation angle. The standard deviation between the predicted and observed UTS values across the two replicate sets of specimens was calculated to be 52.6 MPa, which is 15% of the parent plate tensile strength of 350 MPa and can be regarded as the error of estimate. This error includes effects due to reproducibility and repeatability of the measurement system, welding process and the analysis procedure. Further verification of the predictive model for tensile strength was performed using additional tool geometries which did not form part of the initial experimental matrix.

4. Verification of the Prediction Model

The ability of the proposed model to more generally predict the tensile strength of FS welds was demonstrated using four

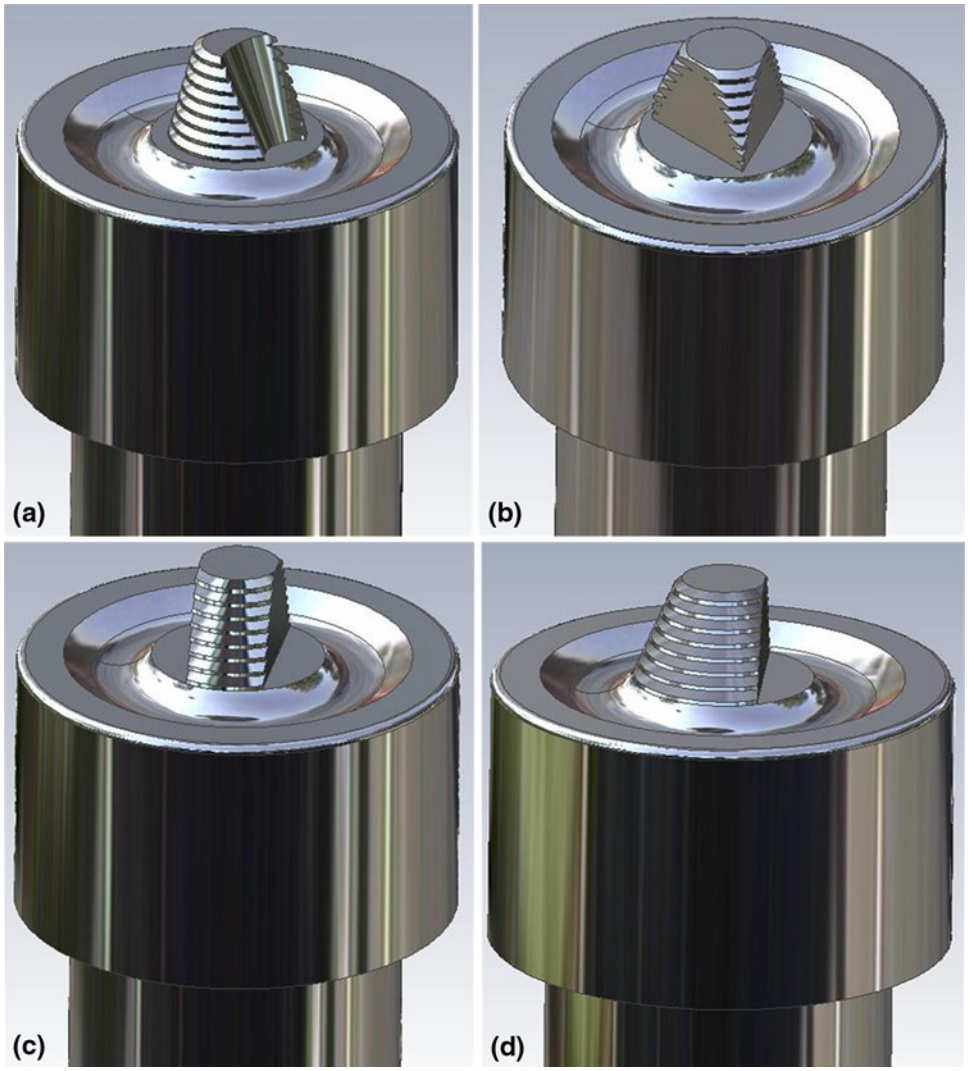

Fig. 5 Additional tool geometries employed to validate the RSM for tensile strength of the welds. (a) Custom Tool 4; (b) SC Tool 1; (c) SC Tool 2; (d) SC Tool 3

additional tool geometries which are illustrated in Fig. 5. These tools did not form part of the initial tool matrix, and welds were made using the same input parameter settings as listed in Table 1. It must be noted that although tests 2 and 5 used the same tool (SC Tool 1), the plunge depth was increased from 0.1 mm in test 2 and 0.2 mm in test 5.

Table 3 gives the measured and predicted values of the tensile strength for these four new tool geometries and summarizes the percentage error at each location along the weld. The error ranges from 1.6 to 48.5%, but the standard deviation over the complete range is only 13%, which indicates that the model is capable of predicting weld tensile strength with reasonable accuracy along a complete weld run of 340 mm.

5. Discussion

The statistically derived prediction of weld tensile strength, based on FS weld process parameters that can be easily depicted using the polar FF diagram, has been shown to yield good results for the strength of welds made with four very different additional tool designs. The error values are within the predicted range of error of 52 MPa, and there is considerable potential to further improve the accuracy of this prediction.

Perhaps the most significant improvement would arise from controlling the downward z-axis force on the tool during welding, which is available with the latest generation of FSW platforms. The data recorded using tool SC1 with increased plunge depth (tests 2 and 5) demonstrate the validity of this statement; the increase in tool shoulder plunge depth resulted in a much higher values of z-force (up from approx. 4 kN to approx. 8 kN), torque (up from 47 to 54 Nm), and tool temperature (up from 490 to 527 °C) giving an average increase in weld tensile strength of 75% (164-287 MPa). Further support for this can be seen in the data for tools SC 2 and SC 4. The SC 2 tool had a much smaller pin volume than the SC 4 tool thus giving rise to lower z-force values. These welds, in particular, gave lower UTS values and illustrate the importance of maintaining a minimum required z-force load on the tool shoulder during welding.

Using this statistical surface response prediction for tensile strength, it is possible to explore efficient ways to optimize the

Table 3 Verification table showing the predicted and measured output responses (UTS), and percentage error for various tools and weld locations

Tool type	Position from weld start, mm	Measured UTS, MPa	Predicted UTS, MPa	%Error UTS, MPa
Custom Tool 4	70	270.11	279.32	3.4
	140	310.12	260.90	15.9
	210	315.59	259.35	17.8
	280	313.25	257.69	17.7
SC Tool 1 plunge depth 0.1 mm	70	176.93	204.29	15.5
	140	168.06	170.81	1.6
	210	167.65	98.61	41.2
	280	143.45	116.45	18.8
SC Tool 2	70	151.92	162.07	6.7
	140	163.31	155.33	4.9
	210	138.29	143.50	3.8
	280	130.62	159.50	22.1
SC Tool 3	70	296.69	304.92	2.8
	140	319.77	253.61	20.7
	210	318.38	242.98	23.7
	280	289.33	200.76	30.6
SC Tool 1 plunge depth 0.2 mm	70	304.17	330.66	8.7
	140	295.92	344.45	48.5
	210	298.12	316.05	6.0
	280	250.00	264.09	5.6

welding process. The complex nature of the interaction between multiple process variables can be visualized using the desirability contour plots provided by statistical software. Desirability functions are useful in response surface methodology as a method to simultaneously optimize a series of parameters which have a quadratic effect on the response variable (weld tensile strength in the present case). Values for the explanatory variables are sought that simultaneously satisfy all of the parametric outcomes. In this study, the desirability level for the weld tensile strength was defined as 0 at 52.6 MPa and 1 at 363.9 MPa. In other words, the desirability values represent the expected minimum and maximum values of the tensile strength prediction with the maximum value having a high desirability of 1. Such contour plots indicate that distinct regions exist where the tensile strength response output meets the preferred conditions. They can also be used in seeking an optimized tool pin geometry, where tool design changes are made so as to keep tensile strength values near the vicinity of the preferred contour regions and to improve weld efficiency.

For instance, the present study indicates that tool temperature has a relatively large range within which it can still produce acceptable weld strength, while *z*-force has a much smaller range to provide acceptable results, indicating that the critical parameter in optimizing the FS weld process is the *z*-force. Controlling the applied *z*-force effectively modifies the heat input and applied torque during welding, but its value is also affected by the tool features. Tool profiles that give high tensile strength and lower *z*-force responses during welding can be regarded as process-efficient tools, as they enable more convenient optimization of other process variables, such as weld feed rate and spindle speed which are related to heat input.

Desirability profile plots are an additional tool to develop optimized tool geometries and weld process conditions. Figure 6 illustrates these desirability profiles for the important process parameters in the RSM discussed in the present article. Each of the graphs in the top row of the figure shows horizontal lines representing the preferred range for tensile strength, lying in a band between 185 MPa and 326 MPa. The mean level of tensile strength (255.5 MPa) corresponds to a desirability level of 0.65, since the full range of tensile strength (not the preferred range) was defined as being from 52.5 MPa (desirability level of 0) to 364 MPa (desirability level of 1). Therefore, when mean values of *z*-force (9.3 kN), torque (58.3 Nm), temperature (558.7°), maximum bending force (3.95 kN), minimum bending force (3.39 kN), and FF rotational angle (34.6°) are substituted into Eq 2, an estimated response of 255.5 MPa will be produced.

The graphs on the bottom row of Fig. 6 provide a horizontal line showing the mean value level of desirability in terms of tensile strength (0.65) and indicate the relative effect of changes in the individual parameters. If it is preferred to improve on this output value of tensile strength (255.5 MPa), then adjustments to the process parameters must be made according to the profile trend lines, e.g., an increasing *z*-force, decreasing torque, or decreasing angle from this mean response will result in an improved weld UTS.

In making changes to tool geometries for optimized FSW, the downward *z*-force loading and parameters described by the FF, especially the rotational angle of the lobed diagram, are the variables that are most effective in influencing the level of interaction between variables and hence the tensile strength of the weld. This statement is supported by the histogram shown in Fig. 4 and also by the desirability profile charts shown in Fig. 6.

This study has considered the relationships between tool design, weld process parameters, and material interactions for a set of fixed conditions. It has to be emphasized that a particular tool may produce different responses when the same set of input parameters are used on different alloys or with a different plate thickness. A series of welding trials are therefore typically required to tailor a specific tool design for a specific application. The present statistical approach will, however, clearly assist in putting process optimization on a firm scientific foundation. A correlation analysis was therefore also performed

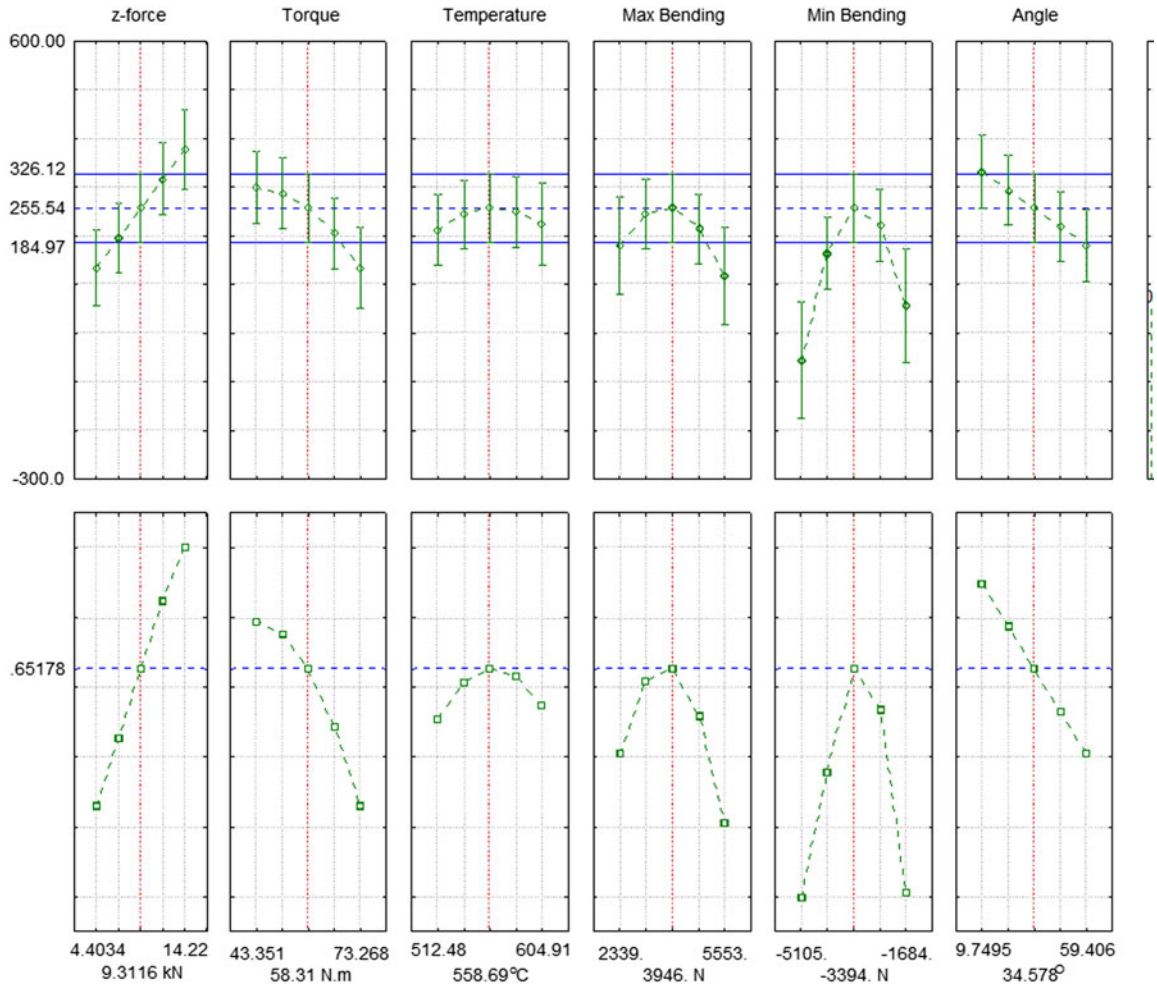

Fig. 6 Profiles for predicted values and desirability of weld tensile strength

Table 4 Correlation coefficients between response variables

Correlation coefficient matrix (*r*-values)							
				Bending force			
	z-Force	Torque	Temperature	Max	Min	Angle	UTS
z-Force	1.00	0.70	0.50	0.47	−0.47	0.12	−0.12
Torque	0.70	1.00	0.40	0.26	−0.34	0.13	−0.14
Temperature	0.50	0.40	1.00	0.17	−0.21	0.07	0.03
Max	0.47	0.26	0.17	1.00	**−0.83**	0.41	**−0.65**
Min	−0.47	−0.34	−0.21	−0.83	1.00	−0.50	**0.70**
Angle	0.12	0.13	0.07	0.41	−0.50	1.00	**−0.57**
UTS	-0.12	−0.14	0.03	−0.65	0.70	−0.57	1.00

of the independent weld process variables (*z*-force, torque, temperature, maximum bending force, minimum bending force, and rotational angle) and the dependent variable of the weld tensile strength. These correlations represent the presence of strong relationships between each variable across a range of different tool designs. In seeking an optimized tool geometry these relationships are important, since a change in one tool feature will result in a change of more than one process response variable, which does not allow separate alterations of variables unless a weak correlation exist between them.

In order to explain this better, a summary of the correlation coefficients for each response variable is provided in Table 4. In this study, the strongest correlation exists between the maximum and minimum bending forces where the correlation coefficient $r = -0.83$. This effectively means that changes in tool design will simultaneously change maximum and

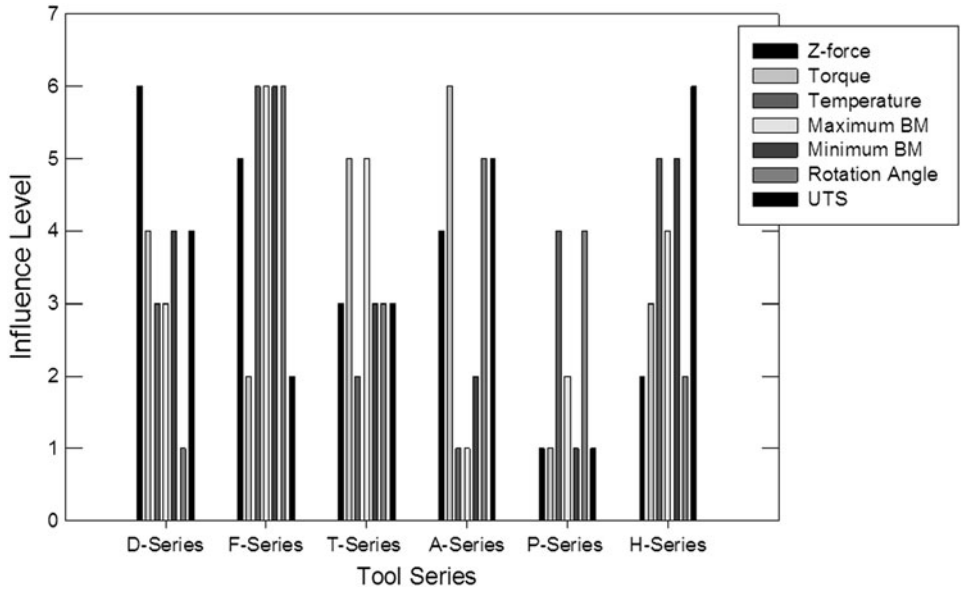

Fig. 7 Bar chart that highlights the characteristic influence behavior of changes in tool profile on specific process responses, e.g., when the pin diameter of the tool is increased (P-Series), it tends to lead to a higher *z*-force during welding. The least influential tool geometry modification on *z*-force response is the flute depth of cut (D-Series). Key to tool series: D, flute depth of cut increase; F, flute angle increase; T, pin taper angle increase; A, amount (number) of flutes increase; P, pin diameter increase; and H, pin thread pitch increase

minimum bending force responses since more than 80% of the maximum force will be affected when the minimum force is changed. The strongest correlation coefficients that exist between weld tensile strength and the other process responses are observed for maximum and minimum bending forces, and the FF rotational angle, as shown in bold in Table 4.

These variables are all properties that are easily and graphically depicted by the FF, and are therefore strongly representative of the plastic zone interactions in the weld region. It is clearly important that special attention is given to these responses during process optimization. It is also clear that the FF could easily be incorporated into a useful GUI for FS process optimization.

Figure 7 provides a bar chart giving a graphical summary of guidelines that can be used during tool geometry modifications. These guidelines indicate the level of influence that tool pin profile changes have on measured process responses, e.g., when the pin diameter of the tool is increased, it tends to lead to a higher *z*-force during welding, while the least influential tool geometry modification on *z*-force response is the flute depth of cut. Modifications made to the diameter of the tool pin will severely influence weld tensile strength.

6. Conclusions

The study presented and discussed in this article has demonstrated the value of a statistical approach to optimizing tool geometry and process parameters in FSW. It has given full details of all the tools used in the study, and indicates some of the reasons as regards why a wide range of tool geometries can produce ‘‘acceptable’’ weld performance in terms of tensile strength when used within a specific window of input parameter settings. It is clear, however, that optimized tensile strength can be obtained via specific combinations of modifications to tool geometry or process parameter settings. Industry normally requires high welding speeds to reduce production costs, and it is therefore essential that modifications in tool geometry can be understood and adapted accordingly in terms of their effects of weld performance.

The model presented in this article was derived from one set of tool geometries and then applied to a further four different geometries, to demonstrate its general utility. The standard deviation between the measured and the predicted tensile strength values for these four additional tool designs was around 13%. This demonstrates that the response surface statistical approach can be very useful for the prediction of weld tensile strength, provided that all the input variables are measured accurately.

The statistical analysis has also indicated that intrinsic plasticity properties of the weld process zone are well represented by the FF diagram (maximum and minimum bending forces, and their rotational angles). The results clearly demonstrate the influence that tool pin profile changes have on measured process responses (Fig. 7).

Future study will aim toward the development of a control algorithm which incorporates the RSM and depicts aspects of this via a GUI which shows the FF. This would allow for making a real-time prediction of the strength of the weld joint.

Acknowledgments

The authors would like to acknowledge the assistance of Dr. Grant Kruger in developing the monitoring and data-logging system, and the financial support from the National Research Foundation (NRF) of South Africa. Dr. Calvin Blignault was the driving force behind this study, and the publication of this article is dedicated to his memory.

References

1. C. Blignault, "A Friction Stir Weld Tool-Force and Response Surface Model Characterizing Tool Performance and Weld Joint Integrity," DTech thesis, Nelson Mandela Metropolitan University, South Africa, 2006
2. D.G. Hattingh, C. Blignault, T.I. van Niekerk, and M.N. James, Characterization of the Influences of FSW Tool Geometry on Welding Forces and Weld Tensile Strength Using an Instrumented Tool, *J. Mater. Process. Technol.*, 2007, **203**(1–3), p 46–57
3. H. Schmidt and J. Hattel, An Analytical Model for Prescribing the Flow Around the Tool Probe in Friction Stir Welding, *Friction Stir Welding and Processing*, K.V. Jata, M. Mahoney, and R. Mishra, Ed., The Minerals, Metals & Materials Society, 2005
4. W.J. Arbegast, Using Process Forces as a Statistical Process Control Tool for Friction Stir Welds, *Friction Stir Welding and Processing*, K.V. Jata, M. Mahoney, and R. Mishra, Ed., The Minerals, Metals & Materials Society, 2005
5. C. Blignault, D.G. Hattingh, G. Kruger, T.I. van Niekerk, and M.N. James, Friction Stir Weld Process Evaluation by Multi-Axial Transducer, *Measurement*, 2008, **41**(1), p 32–43
6. D.G. Hattingh, T.I. van Niekerk, C. Blignault, G. Kruger, and M.N. James, Analysis of the FSW Force Footprint and Its Relationship with Process Parameters to Optimize Weld Performance and Tool Design. Invited Paper (INVITED-2004-01), *IIW J. Weld. World*, 2004, **48**(1–2), p 50–58
7. C. Blignault, "Design, Development and Analysis of the Friction Stir Welding Process," MTech thesis, Port Elizabeth Technikon, South Africa, 2003
8. R.H. Myers and D.C. Montgomery, Response Surface Methodology—Process and Product Optimization Using Designed Experiments, *Wiley Series in Probability and Statistics*, John Wiley, 1995